Disorder-to-chaos transition in the conductance distribution of corrugated waveguides

A. Alcázar-López and J. A. Méndez-Bermúdez
Instituto de Física, Benemérita Universidad Autónoma de Puebla, Apartado Postal J-48, Puebla 72570, Mexico
(Received 15 November 2012; published 6 March 2013)

We perform a detailed numerical study of the distribution of conductances $P(T)$ for quasi-one-dimensional corrugated waveguides as a function of the corrugation complexity (from rough to smooth). We verify the universality of $P(T)$ in both the diffusive ($\langle T\rangle > 1$) and the localized ($\langle T\rangle \ll 1$) transport regimes. However, at the crossover regime ($\langle T\rangle \sim 1$), we observe that $P(T)$ evolves from the surface-disorder to the bulk-disorder theoretical predictions for decreasing complexity in the waveguide boundaries. We explain this behavior as a transition from disorder to deterministic chaos since in the limit of smooth boundaries the corrugated waveguides are, effectively, linear chains of chaotic cavities.

DOI: 10.1103/PhysRevE.87.032904 PACS number(s): 05.45.−a, 73.23.−b, 71.30.+h, 42.25.Dd

I. INTRODUCTION

In studies of wave propagation through disordered wires two setups are mostly considered: bulk-disordered and surface-disordered waveguides. In both cases it is possible to discern between diffusive (metallic) and localized (insulating) transport regimes by comparing the wire length L with the mean-free path ℓ and the localization length ξ; i.e., wave diffusion takes place when $\ell \ll L \ll \xi$, while localization is observed for $\xi \ll L$.

From the analytical point of view, both disorder setups have been successfully approached. On the one hand, transport through bulk-disordered waveguides is well described by the Fokker-Planck approach of Dorokhov, Mello, Pereyra, and Kumar (DMPK) [1–6], and by the field-theoretic approach of Efetov and Larkin, which leads to a supersymmetric nonlinear σ model [7–9]. In fact, these two approaches were shown to be equivalent in Ref. [10]. In addition, in Ref. [11], the distribution of conductances $P(T)$ in the full diffusive-to-localized crossover was derived, in the frame of the supersymmetric approach, for waveguides with broken time-reversal invariance [12]. On the other hand, transport through surface-disordered wires has been properly characterized by the Fokker-Planck approach developed by Froufe-Perez, Yepez, Mello, and Saenz (FYMS) [13]. Other analytical approaches to transport through surface-disordered wires are also available in Refs. [14,15].

Furthermore, for both setups, $P(T)$ evolves from a Gaussian shape (deep in the diffusive regime) to a log-normal shape (deep in the localized regime). However, at the crossover between diffusive and localized regimes, the form of $P(T)$ is highly nontrivial [6,13,16–23] and importantly depends on the type of disorder (bulk or surface). Moreover, the DMPK approach and the FYMS approach provide accurate predictions for $P(T)$ at the crossover regime for the corresponding setups of disorder [6,13,16–20].

In this paper we numerically study $P(T)$ for a model of quasi-one-dimensional surface-disordered waveguides with tunable corrugation complexity: from rough to smooth. Here, we concentrate on waveguides with time-reversal invariance. We define the corrugated surface of our disordered wire as a sum of harmonics with random amplitudes. In the rough limit (large number of harmonics) the waveguide effectively shows surface disorder; so, it is equivalent to the steplike corrugated waveguide model used in Refs. [16–19]. On the other hand, in the smooth limit (few harmonics) the waveguide can be considered as a linear chain of attached chaotic cavities. Interestingly, the transport properties of a waveguide constructed as a linear chain of chaotic cavities [9,24,25] are equivalent to those of a bulk-disordered wire [10]. Then, by decreasing the corrugation complexity of our surface corrugated waveguide, we expect to observe, at the diffusive-to-localized transition regime, a transition in the form of $P(T)$ from the surface-disorder FYMS to the bulk-disorder DMPK predictions.

The organization of this paper is as follows. In the next section we define the waveguide model we use as well as the scattering setup. In Sec. III, by extracting ℓ and ξ from curves of the average resistance and average logarithm of conductance as a function of L, respectively, we define the diffusive and localized transport regimes for our corrugated waveguides. Then we study in detail the distribution of conductances $P(T)$ as a function of the corrugation complexity in both regimes, diffusive and localized, as well as at the crossover regime. Finally, Sec. IV is left for conclusions.

II. MODEL

The model we shall use in our study is a waveguide formed by attaching L two-dimensional cavities. Each cavity of length L_x is defined by two hard walls: one flat at $y = 0$ and a corrugated one given by $y = d + \epsilon f(x)$. Here d is the average width of the cavity and ϵ is the corrugation amplitude. Since we are interested in studying the transport properties of waveguides as a function of the complexity of the corrugated boundary we choose

$$f(x) = \sum_{n=1}^{N_T} A_n \cos\left(\frac{2\pi n}{L_x}x\right), \tag{1}$$

where A_n are random numbers drawn from a flat distribution in the range $[-1,1]$. This form for $f(x)$ allows us to choose the desired degree of complexity of the corrugated waveguide boundary: from rough, $N_T \sim 20$, to smooth, $N_T \sim 1$ (see Fig. 1). It is important to stress that once the parameters L_x, d, ϵ, and N_T are fixed we randomly generate (through different values of A_n) L different cavities that we attach to form a nonperiodic waveguide [26,27]. To this end the minimal N_T we use is 2.

We note that depending on the values of the parameters (L_x, d, ϵ, and N_T), the classical (or ray) dynamics in each of the cavities can yield mixed or full chaos. However, here we

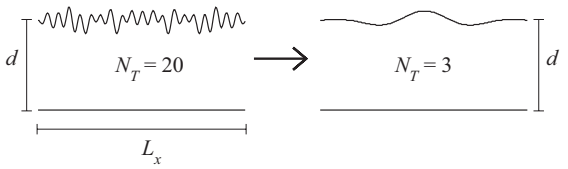

FIG. 1. Examples of cavities used to form corrugated waveguides. Here we show one realization of cavities with $N_T = 20$ and $N_T = 3$. In our study we go from $N_T = 18$ to $N_T = 2$.

consider only the case of full chaos [28]: $\epsilon d N_T / L_x^2 > 0.01$. Then, below we use $L_x = 2\pi$, $d = L_x/2$, and $\epsilon = L_x/20$. This set of parameters produces full chaos for any $N_T \geqslant 1$. Finally, note that all lengths, here and below (including ℓ, ξ, and L), are given in units of L_x.

We open the waveguide of length L defined above by attaching two semi-infinite collinear flat leads of width d to its left and right ends. The leads support plane waves with energy $E = (\hbar^2/2\mathbf{m})[k_m^2 + (m\pi/d)^2]$, where k_m and $m\pi/d$ are, respectively, the longitudinal and transversal components of the total wave vector $K = \sqrt{2\mathbf{m}E}/\hbar$. Then, using finite element methods (see, e.g., [29,30]) we compute the scattering matrix, S matrix, which has the form

$$S = \begin{pmatrix} t & r' \\ r & t' \end{pmatrix},$$

where t, t', r, and r' are $M \times M$ transmission and reflection matrices. Here, M is the highest mode given by the largest m beyond which the longitudinal wave vector $k_m = [2\mathbf{m}E/\hbar^2 - (m\pi/d)^2]^{1/2}$ becomes complex. Then, once the S matrix is known we calculate the dimensionless conductance from [31]

$$T = \mathrm{Tr}(tt^\dagger). \tag{2}$$

With this definition, the conductance can take values in the interval $[0, M]$.

The experimental realization of a scattering setup similar to ours has been recently reported in Ref. [32]. However, we notice that in numerical simulations of transport through surface-disordered wires, steplike corrugated waveguides are more often used [16–19,33–35], among others [13,36]. We also note that here we concentrate on the case of small number of open modes, $M = [2,9]$; the case of $M \gg 1$ has been recently addressed in Ref. [35].

III. RESULTS

A. Diffusive and localized regimes

In order to identify the diffusive and localized transport regimes in our corrugated waveguides, in Fig. 2 we plot the average resistance $\langle 1/T \rangle$ and the average logarithm of conductance $\langle \ln T \rangle$ as a function of L for waveguides with $N_T = 18$, 8, 3, and 2.

For disordered wires, it is well established that (i) for relatively short wire lengths the resistance increases linearly with L as [16,36–38]

$$\left\langle \frac{1}{T} \right\rangle = \frac{1}{M} + \frac{L}{M\ell}, \tag{3}$$

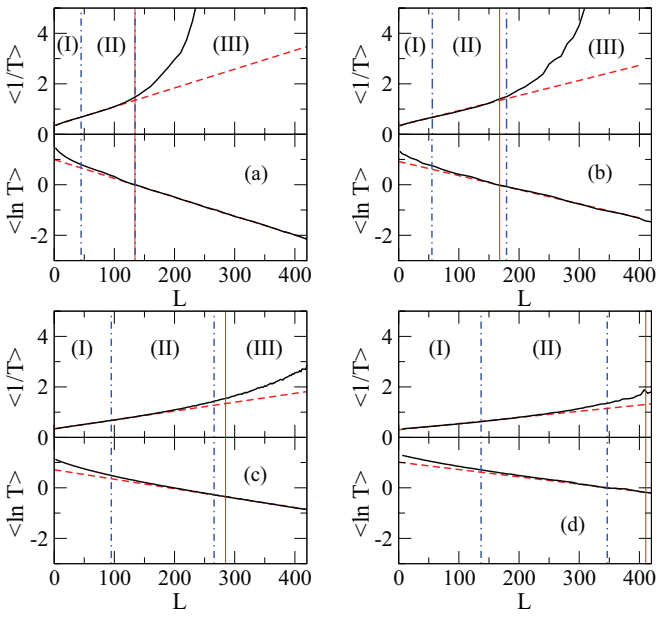

FIG. 2. (Color online) Average resistance $\langle 1/T \rangle$ (upper panels) and average logarithm of conductance $\langle \ln T \rangle$ (lower panels) as a function of the length L of corrugated waveguides with (a) $N_T = 18$, (b) 8, (c) 3, and (d) 2 (black full lines). To average, 10^4 waveguide realizations were used. The waveguides support $M = 3$ open modes. Red dashed lines are best fittings of $\langle 1/T \rangle$ [$\langle \ln T \rangle$] with Eq. (3) [Eq. (4)] for small [large] L. The extracted (ℓ,ξ) are approximately equal to (a) (44.77,134.38), (b) (55.88,179.28), (c) (94.97,265.78), and (d) (136.88,346.61). Blue dot-dashed vertical lines indicate the positions of ℓ and ξ which delimit the transport regimes: quasiballistic (I), diffusive (II), and localized (III). Red vertical lines mark the value of $M\ell$.

while (ii) for relatively large wire lengths the conductance decays exponentially with L in the form [16,36,39,40]

$$\langle \ln T \rangle \propto -\frac{L}{\xi}. \tag{4}$$

We extract ℓ and ξ from Fig. 2 by performing fittings of the data with Eqs. (3) and (4), respectively (see red dashed lines). In Fig. 2 we also indicate, with blue dot-dashed vertical lines, the positions of the obtained ℓ and ξ. From this figure, it is clear that both ℓ and ξ decrease by increasing N_T; equivalently, the mean-free path and the localization length increase when the disorder decreases. Therefore, in Fig. 2 we label as (II) and (III) the diffusive and localized regimes, respectively. Additionally, we identify with (I) the quasiballistic regime $L < \ell$, which we will not explore here.

It is also interesting to mention that we found that relation $\xi \approx M\ell$ (see, for example, [17,19]) works well only when the surface corrugation is complex enough, i.e., for $N_T \geqslant 7$ (see upper panels of Fig. 2). When $N_T \to 1$ we observe that $\xi < M\ell$ (see lower panels of Fig. 2). In any case the diffusive regime is clearly discernible in our calculations for all the values of M and N_T we used here.

Note that to construct Fig. 2 we have used waveguides supporting $M = 3$ open modes. [Here and below, when showing results for different values of M we always fix the energy such that $K = \pi(M + 1/2)/d$.] We obtained similar plots for other values of M. However, by increasing M the

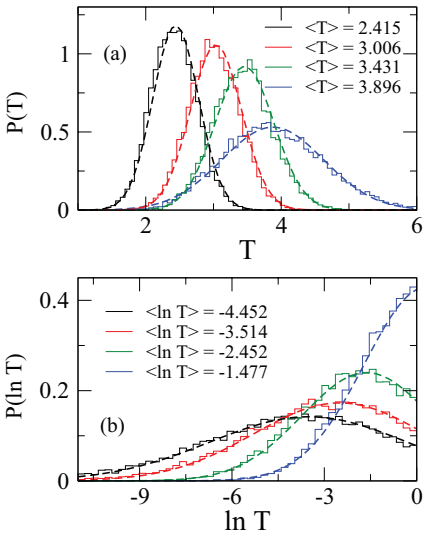

FIG. 3. (Color online) Conductance probability distributions (a) $P(T)$ and (b) $P(\ln T)$ for corrugated waveguides with $N_T = 18$, 8, 3, and 2 (from left to right) in the (a) diffusive and (b) localized regimes. 10^4 values of T were used to construct each histogram. The waveguides support $M = 9$ open modes. Dashed lines are (a) Gaussian and (b) log-normal distribution functions characterized by the values of (a) $\langle T \rangle$ and (b) $\langle \ln T \rangle$ reported in the corresponding panels.

values of ℓ and ξ decrease and, as a consequence, the regimes (I) and (II) become narrower. For $M = 9$, the highest M we explored, the quasiballistic regime is hardly visible in the scale of Fig. 2. In the following figures we will use values of M different from 3 to emphasize that our results do not depend on the number of open modes, once the transport regimes are well determined.

Then, in Fig. 3, we verify the predictions for the conductance probability distribution function in the diffusive and localized regimes. As clearly shown in this figure, where $M = 9$ open modes were considered, $P(T)$ has a well defined Gaussian shape in the diffusive regime [Fig. 3(a)], while $P(\ln T)$ has the log-normal form in the localized regime [Fig. 3(b)]. We know that the results reported in Fig. 3 are already expected and thus it may seem unnecessary to show them. However, we decided to present them in order to stress that the transport properties, exemplified here by the form of $P(T)$, of rough and smooth corrugated waveguides are in fact similar except at the crossover regime, as will be shown below.

B. Crossover regime

As already anticipated, we have found that the most interesting result for the distribution of conductances appears at the crossover regime, where $\langle T \rangle \sim 1$. Here, we observe that the shape of $P(T)$ does depend on the waveguide corrugation complexity. To show this, in Fig. 4 we plot $P(T)$ for corrugated

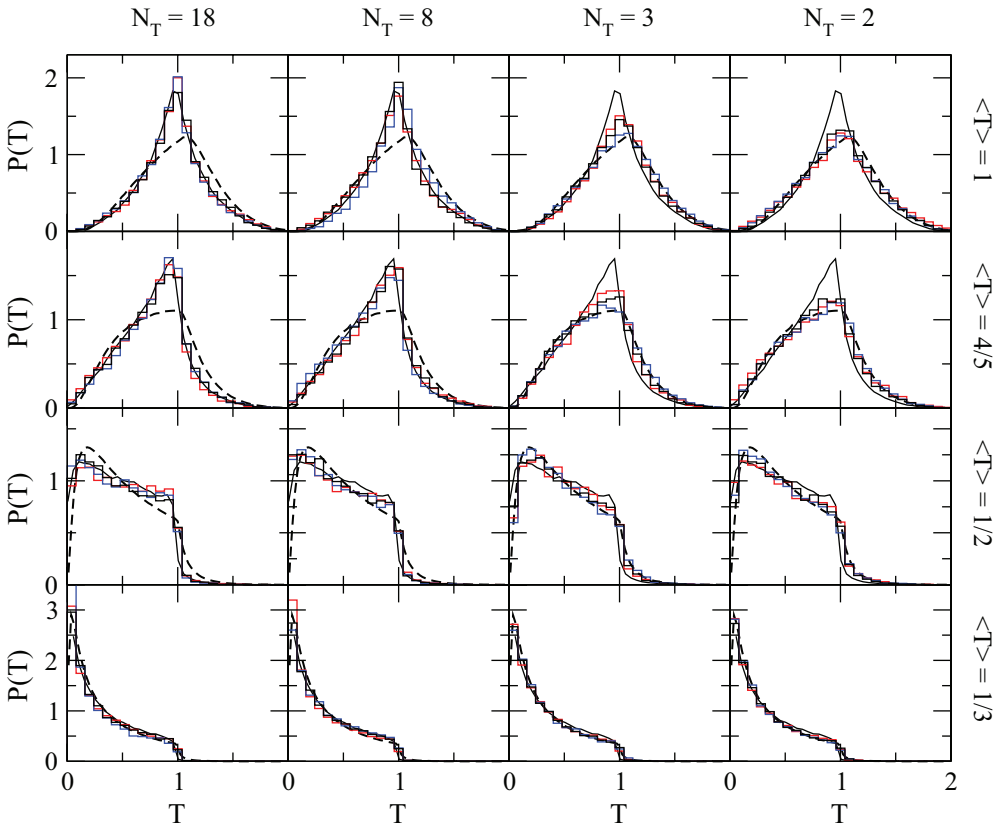

FIG. 4. (Color online) Conductance probability distributions $P(T)$ for corrugated waveguides with $N_T = 18$, 8, 3, and 2 (columns) for $\langle T \rangle = 1$, 4/5, 1/2, and 1/3 (rows). Each panel contains three histograms corresponding to waveguides with $M = 5$, 7, and 8. 10^4 values of T were used to construct each histogram. Continuous and dashed lines are the surface-disorder FYMS and the bulk-disorder DMPK predictions for $P(T)$, taken from [13,18], respectively.

waveguides with $N_T = 18$, 8, 3, and 2 (columns) for some values of $\langle T \rangle$ (for comparison purposes in Fig. 4 we chose the same values of $\langle T \rangle$ used in [13,16–19]). As a reference, we also include the surface-disorder FYMS and the bulk-disorder DMPK predictions for $P(T)$. In each panel we plot three histograms corresponding to waveguides supporting $M = 5$, 7, and 8 open modes. Note that for large N_T, in our case $N_T = 18$ [41], the shapes of the numerically obtained $P(T)$ are well described by the FYMS prediction for surface-disordered waveguides, as expected (see panels in the leftmost column of Fig. 4). However, once the waveguide corrugation complexity is decreased, important deviations appear. Moreover, when $N_T = 2$, $P(T)$ fully coincides with the DMPK prediction for bulk-disordered waveguides (see panels in the rightmost column of Fig. 4). This fact is more evident for $\langle T \rangle = 1$ and $4/5$ where the differences between FYMS and DMPK predictions are easily distinguishable.

So, we observe an effective and smooth evolution in the form of $P(T)$, from the surface-disorder FYMS to the bulk-disorder DMPK predictions, as a function of the (decreasing) waveguide corrugation complexity N_T. We understand this result in the following simple way. In the limit $N_T \to 1$ our waveguide can be considered as a linear chain of coupled chaotic cavities, each one defined by the cosine billiard [42]. Then, the model of quantum dots in series of Iida, Weidenmuller, and Zuk applies [24]. Moreover, this model reduces to a supersymmetric nonlinear σ model [7–9] which turns out to be equivalent to the DMPK approach [10]. That is, while FYMS describes well the limit $N_T \gg 1$ of our corrugated waveguide, DMPK should describe the limit $N_T \to 1$, as we in fact observe in Fig. 4. Therefore, our waveguide model shows a disorder-to-chaos transition in the shape of the conductance distribution.

Finally, we want to add that the parameters used in Refs. [16–19], translated to our symbols, are [43]: $d/\epsilon = 7 - 13.25$ (here we used $d/\epsilon = 10$) and $N_T \approx 7$. Then, since we are observing well developed surface-disorder FYMS transport properties in our corrugated waveguides for $N_T \geqslant 8$, there is no contradiction between our results and those presented in Refs. [16–19]. Moreover, we think that it would be interesting to explore the limit where the step length, in the steplike corrugated waveguide model of Refs. [16–19], becomes of the order of the waveguide width, which is somehow equivalent to the limit $N_T \to 1$ in our waveguide model.

IV. CONCLUSIONS

We have studied the distribution of conductances $P(T)$ for a quasi-one-dimensional corrugated waveguide with tunable corrugation complexity: from rough, $N_T = 18$, to smooth, $N_T = 2$. We verified that both the mean free path and the localization length decrease for increasing N_T. Also, we confirmed that $P(T)$ and $P(\ln T)$ have the Gaussian and log-normal shapes in the diffusive ($\langle T \rangle > 1$) and localized ($\langle T \rangle \ll 1$) transport regimes, respectively.

At the crossover between the diffusive and the localized regime $\langle T \rangle \sim 1$, we reported that $P(T)$ monotonously evolves from the surface-disorder FYMS (when $N_T = 18$) to the bulk-disorder DMPK (when $N_T = 2$) predictions for decreasing N_T. We understood this behavior as a consequence of the underlying deterministic dynamical chaos since the waveguides having smooth boundaries (i.e., when $N_T \to 1$) are effectively linear chains of attached chaotic cavities.

We believe that our results, as well as our model of corrugated wires with tunable corrugation complexity, may stimulate further analytical and numerical studies on the transport properties at the diffusive-to-localized transition regime.

ACKNOWLEDGMENTS

We acknowledge support form VIEP-BUAP grant MEBJ-EXC12-G and Fondo Institucional PIFCA 2012 (BUAP-CA-169).

[1] O. N. Dorokhov, Pis'ma Zh. Eksp. Teor. Fiz. **36**, 259 (1982) [JETP Lett. **36**, 318 (1982)].
[2] P. A. Mello, P. Pereyra, and N. Kumar, Ann. Phys. (NY) **181**, 290 (1988).
[3] P. A. Mello, Phys. Rev. Lett. **60**, 1089 (1988).
[4] P. A. Mello and A. D. Stone, Phys. Rev. B **44**, 3559 (1991).
[5] A. M. S. Macedo and J. T. Chalker, Phys. Rev. B **46**, 14985 (1992).
[6] P. A. Mello and N. Kumar, *Quantum Transport in Mesoscopic Systems* (Oxford University Press, Oxford, 2004).
[7] K. B. Efetov and A. I. Larkin, Zh. Eksp. Teor. Fiz. **85**, 764 (1983) [Sov. Phys. JETP **58**, 444 (1983)].
[8] K. B. Efetov, Adv. Phys. **32**, 53 (1983).
[9] A. D. Mirlin, A. Müller-Groeling, and M. R. Zirnbauer, Ann. Phys. (NY) **236**, 325 (1994).
[10] P. W. Brouwer and K. Frahm, Phys. Rev. B **53**, 1490 (1996).
[11] Y. V. Fyodorov, Pis'ma Zh. Eksp. Teor. Fiz. **78**, 286 (2003) [JETP Lett. **78**, 250 (2003)].
[12] The scattering setup considered in Ref. [11] consists of a single-mode lead attached to one side of the waveguide and a lead supporting very many modes attached to the other side.
[13] L. S. Froufe-Perez, M. Yepez, P. A. Mello, and J. J. Saenz, Phys. Rev. E **75**, 031113 (2007); M. Yepez, Ph.D. thesis, Universidad Nacional Autónoma de México, Mexico, 2009.
[14] N. M. Makarov, A. V. Moroz, and V. A. Yampol'skii, Phys. Rev. B **52**, 6087 (1995); N. M. Makarov and Y. V. Tarasov, J. Phys.: Condens. Matter **10**, 1523 (1998).
[15] F. M. Izrailev, N. M. Makarov, and M. Rendon, Phys. Rev. B **72**, 041403(R) (2005); **73**, 155421 (2006); M. Rendon, F. M. Izrailev, and N. M. Makarov, *ibid.* **75**, 205404 (2007); M. Rendon, N. M. Makarov, and F. M. Izrailev, Phys. Rev. E **83**, 051124 (2011).
[16] A. Garcia-Martin, J. A. Torres, J. J. Saenz, and M. Nieto-Vesperinas, Appl. Phys. Lett. **71**, 1912 (1997).
[17] A. Garcia-Martin and J. J. Saenz, Phys. Rev. Lett. **87**, 116603 (2001).

[18] L. S. Froufe-Perez, P. Garcia-Mochales, P. A. Serena, P. A. Mello, and J. J. Saenz, Phys. Rev. Lett. **89**, 246403 (2002).
[19] A. Garcia-Martin and J. J. Saenz, Waves Random Complex Media **15**, 229 (2005).
[20] V. A. Gopar, K. A. Muttalib, and P. Wölfle, Phys. Rev. B **66**, 174204 (2002).
[21] A. Cresti, R. Farchioni, and G. Grosso, Eur. Phys. J. B **46**, 133 (2005).
[22] V. Plerou and Z. Wang, Phys. Rev. B **58**, 1967 (1998).
[23] P. Markos, Phys. Rev. B **65**, 104207 (2002).
[24] S. Iida, H. A. Weidenmüller, and J. A. Zuk, Phys. Rev. Lett. **64**, 583 (1990); Ann. Phys. (NY) **200**, 219 (1990).
[25] C. W. J. Beenakker, Rev. Mod. Phys. **69**, 731 (1997).
[26] The periodic version of our corrugated waveguide has already been used in F. M. Izrailev, J. A. Mendez-Bermudez, and G. A. Luna-Acosta, Phys. Rev. E **68**, 066201 (2003); J. A. Mendez-Bermudez, G. A. Luna-Acosta, and F. M. Izrailev, Physica E **22**, 881 (2004) to study the properties of eigenstates in the transition from disorder to deterministic chaos.
[27] The transport properties of a waveguide similar to ours, in the smooth limit, but periodic have been studied in F. Barra, V. Pagneux, and J. Zuñiga, Phys. Rev. E **85**, 016209 (2012); J. Zuñiga, Ph.D. thesis, Universidad de Chile, Santiago, 2011.
[28] A. J. Martinez-Mendoza, J. A. Mendez-Bermudez, G. A. Luna-Acosta, and N. Atenco-Analco, Rev. Mex. Fis. S **58**, 6 (2012).
[29] G. A. Luna-Acosta, J. A. Mendez-Bermudez, P. Seba, and K. N. Pichugin, Phys. Rev. E **65**, 046605 (2002).
[30] J. A. Mendez-Bermudez, G. A. Luna-Acosta, P. Seba, and K. N. Pichugin, Phys. Rev. E **66**, 046207 (2002).
[31] R. Landauer, IBM J. Res. Dev. **1**, 223 (1957); **32**, 336 (1988); M. Buttiker, Phys. Rev. Lett. **57**, 1761 (1986); IBM J. Res. Dev. **32**, 317 (1988).
[32] O. Dietz, H.-J. Stöckmann, U. Kuhl, F. M. Izrailev, N. M. Makarov, J. Doppler, F. Libisch, and S. Rotter, Phys. Rev. B **86**, 201106(R) (2012).
[33] J. Feist, A. Backer, R. Ketzmerick, S. Rotter, B. Huckestein, and J. Burgdorfer, Phys. Rev. Lett. **97**, 116804 (2006); J. Feist, A. Backer, R. Ketzmerick, J. Burgdorfer, and S. Rotter, Phys. Rev. B **80**, 245322 (2009).
[34] A. Garcia-Martin, J. A. Torres, J. J. Saenz, and M. Nieto-Vesperinas, Phys. Rev. Lett. **80**, 4165 (1998); A. Garcia-Martin, T. Lopez-Ciudad, J. J. Saenz, and M. Nieto-Vesperinas, *ibid.* **81**, 329 (1998); A. Garcia-Martin, J. J. Saenz, and M. Nieto-Vesperinas, *ibid*. **84**, 3578 (2000).
[35] J. Feilhauer and M. Mosko, Phys. Rev. B **83**, 245328 (2011).
[36] J. A. Sanchez-Gil, V. Freilikher, I. V. Yurkevich, and A. A. Maradudin, Phys. Rev. Lett. **80**, 948 (1998); J. A. Sanchez-Gil, V. Freilikher, A. A. Maradudin, and I. V. Yurkevich, Phys. Rev. B **59**, 5915 (1999).
[37] T. M. Nieuwenhuizen and J. M. Luck, Phys. Rev. E **48**, 569 (1993); A. Mosk, T. M. Nieuwenhuizen, and C. Barnes, Phys. Rev. B **53**, 15914 (1996).
[38] T. N. Todorov, Phys. Rev. B **54**, 5801 (1996).
[39] P. W. Anderson, D. J. Thouless, E. Abrahams, and D. S. Fisher, Phys. Rev. B **22**, 3519 (1980); P. W. Anderson, *ibid*. **23**, 4828 (1981).
[40] P. A. Lee, A. D. Stone, and H. Fukuyama, Phys. Rev. B **35**, 1039 (1987).
[41] We have verified that our conclusions do not change when considering larger values of N_T.
[42] G. A. Luna-Acosta, K. Na, L. E. Reichl, and A. Krokhin, Phys. Rev. E **53**, 3271 (1996); L. E. Reichl, *The Transition to Chaos* (Springer-Verlag, New York, 2004).
[43] Evidently, the parameter N_T does not exist in the step-like corrugated waveguide model of Refs. [16–19]. However, there the step length l plays the role of the inverse of N_T in our waveguide model. In fact, by discretizing our smooth cosinelike corrugation we could write $l \equiv L_x/2N_T$.